scientific reports

Check for updates

OPEN

High bandwidth performance of newly designed multimode W-type microstructured plastic optical fibers with graded-index core distribution

Ana Simović[1], Branko Drljača[2], Milan S. Kovačević[1], Ljubica Kuzmanović[1], Alexandar Djordjevich[3], Konstantinos Aidinis[4,5], Changyuan Yu[6], Xiong Deng[7] & Svetislav Savović[1]✉

A new design of multimode W-type (doubly clad) microstructured plastic optical fiber (mPOF) with graded-index (GI) distribution of the core is proposed, along with a methodology for examining transmission along it. The power flow equation's (PFE) numerical solution yields the transmission properties of the W-type GI mPOF. We have demonstrated that the coupling length L_c at which an equilibrium mode distribution (EMD) is reached in W-type GI mPOF is shorter than the length experimentally found for the conventional singly- clad (SC) GI POF. This results from leaky mode losses, which lower the length L_c in W-type GI mPOF by lowering the amount of higher guided modes engaged in the coupling process. As a result, the bandwidth of W-type GI mPOF significantly increases. It is noteworthy that, when compared to the experimental bandwidth of commercially available conventional POFs, the bandwidth of the W-type GI mPOF proposed in this work is noticeably higher. Consequently, the bandwidth performance of short-haul communication lines may be significantly improved by using such a designed W-type GI mPOF.

Keywords W-type microstructured POF, Graded-index POF, Power flow equation, Equilibrium mode distribution, Bandwidth

In order to facilitate a wide range of services, including the Internet of Things, augmented reality, virtual reality, video streaming, and online gaming with very high data and low latency, fifth-generation (5G) and sixth-generation (6G) communication are needed. Nevertheless, lower-band communication finds it difficult to accommodate the high data rate transmission due to the already congested current band. POFs have a variety of applications across different industries due to their unique properties, such as short-range data communication, illumination, sensing, medical imaging, automotive applications, high-power delivery, consumer electronics and safety equipment. Overall, the use of POFs continues to grow as technology advances and new applications are discovered. Their flexibility, durability, and resistance to electromagnetic interference make them an attractive choice for various industries. The advantage of microstructured plastic optical fiber (mPOF) over traditional POF is the ability to adjust air-hole diameters and pitches with greater flexibility, without the need for complex doping procedures as with regular POF.

Optical fiber bandwidth can be increased by different multiplexing, more sophisticated techniques, and appropriate refractive index design[1–5]. Because of this, it is critical to ascertain the circumstances in which an optical fiber has the largest bandwidth, i.e., to develop models that can predict and ascertain how fiber design

[1]Faculty of Science, University of Kragujevac, R. Domanovića 12, Kragujevac 34000, Serbia. [2]Faculty of Sciences and Mathematics, University of Priština in Kosovska Mitrovica, Lole Ribara 29, Kosovska Mitrovica, Serbia. [3]Department of Mechanical Engineering, City University of Hong Kong, 83 Tat Chee Avenue, Kowloon, Hong Kong, China. [4]Department of Electrical and Computer Engineering, Ajman University, P.O. Box 346, Ajman, United Arab Emirates. [5]Center of Medical and Bio-allied Health Sciences Research, Ajman University, P.O. Box 346, Ajman, United Arab Emirates. [6]Department of Electrical and Electronic Engineering, The Hong Kong Polytechnic University, Pokfulam, Hong Kong SAR, China. [7]School of Information Science and Technology, Southwest Jiaotong University, Chengdu, China. ✉email: savovic@kg.ac.rs

characteristics affect bandwidth. Previous work on modeling and experimental investigation of the transmission characteristics of various multimode optical fiber types by a number of research teams demonstrated that the transmission characteristics of the fibers can be greatly enhanced by appropriately adjusting the fiber's parameters[6–18]. The obtained results demonstrated that singly-clad (SC) graded-index (GI) POFs have a substantially lower modal dispersion than SC step-index (SI) POFs because of their gradually decreasing core refractive index with a radial distance from the fiber axis[19]. One anticipates that the proposed double clad W-type GI mPOF will perform better in terms of fiber bandwidth than all other currently available conventional POFs and mPOFs as the modal dispersion of double-clad W-type POF is less than that of SC POF[20]. Moreover, an advantage of a mPOF is its increased flexibility in modifying its geometric parameters, in contrast to conventional POF, which is based on core and cladding(s) with varying doping levels[19].

The optical power distribution launched into a multimode optical fiber evolves gradually along the fiber length due to mode coupling effects. This process alters the expected beam characteristics, including the far-field radiation pattern. The far-field pattern of a fiber depends on the initial launch conditions, the fiber's physical properties, and its length. When light is launched at a specific angle or radial offset relative to the fiber axis, it produces a well-defined ring-shaped radiation pattern at the output of short fibers. However, due to mode coupling, the edges of this ring become increasingly blurred with longer fiber lengths. Up to a certain point, known as the "coupling length" L_c, this blurring intensifies with distance, and the ring pattern gradually transitions L_c, the fiber reaches an equilibrium mode distribution (EMD), where the output no longer exhibits ring patterns regardless of the launch angle. Although the disk-shaped distribution may still depend on the launch conditions, EMD signifies that mode coupling is nearly complete. At a distance $z_s > L_c$ from the fiber input, the disk patterns resulting from various launch angles converge into a single, uniform distribution across the fiber cross-section. This state, known as steady-state distribution (SSD), represents the full completion of mode coupling, rendering the output light distribution independent of the input launch conditions."

There is no commercial modeling tool available for researching highly multimode microstructured optical fibers (MOFs) transmission characteristics. This study investigates the transmission characteristics of W-type GI mPOF by numerically solving the time-independent power flow equation (TI PFE) in order to get over this issue. More precisely, we looked into how different configurations of W-type mPOFs with GI distribution of the core affect bandwidth as well as the length at which an EMD and SSD are obtained. We proposed that the air holes in this optical fiber's core and cladding be placed in a grid of triangles with regular pitch Λ (see Fig. 1).

Time-independent PFE

The TI PFE for multimode GI fibers is given as[13]:

$$\frac{\partial P(m,\lambda,z)}{\partial z} = -\alpha(m,\lambda)P(m,\lambda,z) + \frac{1}{m}\frac{\partial}{\partial m}\left(md(m,\lambda)\frac{\partial P(m,\lambda,z)}{\partial m}\right) \tag{1}$$

where $P(m,\lambda,z)$ is power in the m-th principal mode (modal group), z is coordinate along the fiber axis, $d(m,\lambda)$ is mode coupling coefficient (assumed constant D)[14], $\alpha(m,\lambda) = \alpha_0(\lambda) + \alpha_d(m,\lambda)$ is modal attenuation, where α_0 represents conventional losses (absorption and scattering). The term α_0 leads only to a multiplier $\exp(-\alpha_0 z)$ in the solution and can be neglected.

The RI profile of W-type optical fibers with GI distribution of the core (see Fig. 1(b)) can be written as follows:

$$n(r,\lambda) = \begin{cases} n_{co}(\lambda)\left[1 - \Delta_q(\lambda)\left(\frac{r}{a}\right)^g\right]^{1/2} & (0 \leqslant r \leqslant a) \\ n_q & (a < r \leqslant a + \delta a) \\ n_p & (a + \delta a < r \leqslant \frac{b}{2}) \end{cases} \tag{2}$$

where g is core index exponent, a is core radius, δa is intermediate layer width, b is fiber diameter, $n_{co}(\lambda)$ is the maximum RI of the core (measured at the fiber axis), n_q and n_p are RI of intermediate layer and cladding, respectively, $\Delta_q = (n_{co} - n_q)/n_{co}$ is relative index difference between core and intermediate layer. The maximum principal mode number $M(\lambda)$ given as[21]:

$$M(\lambda) \equiv m_q = \sqrt{\frac{g\Delta_q(\lambda)}{g+2}}akn_{co}(\lambda) \tag{3}$$

where $k = 2\pi/\lambda$ is the free-space wave number. Gaussian launch-beam distribution (LBD) $P_0(\theta,\lambda,z=0)$ can be transformed into $P_0(m,\lambda,z=0)$ (one needs $P_0(m,\lambda,z=0)$ to numerically solve the PFE (1)), using the following relationship[22]:

$$\frac{m}{M(\lambda)} = \left[\left(\frac{\Delta r}{a}\right)^g + \frac{\theta^2}{2\Delta_q(\lambda)}\right]^{(g+2)/2g} \tag{4}$$

where Δr is radial distance (radial offset) between the position of the maximum of the LBD and the core center, θ is the propagation angle with respect to the core axis and $\Delta_q = (n_{co} - n_q)/n_{co}$ is the relative RI difference between the core and intermediate layer. Attenuation constant of leaky modes $m_p < m < m_q$ is given as[23]:

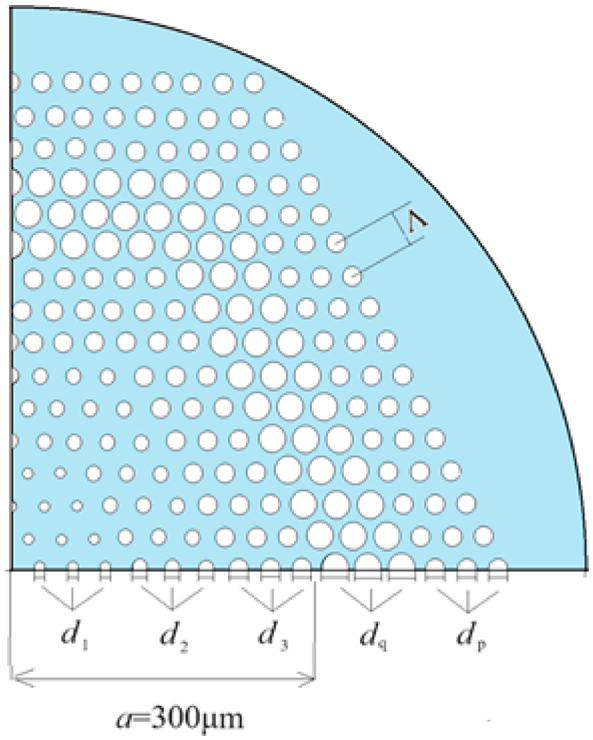

(a)

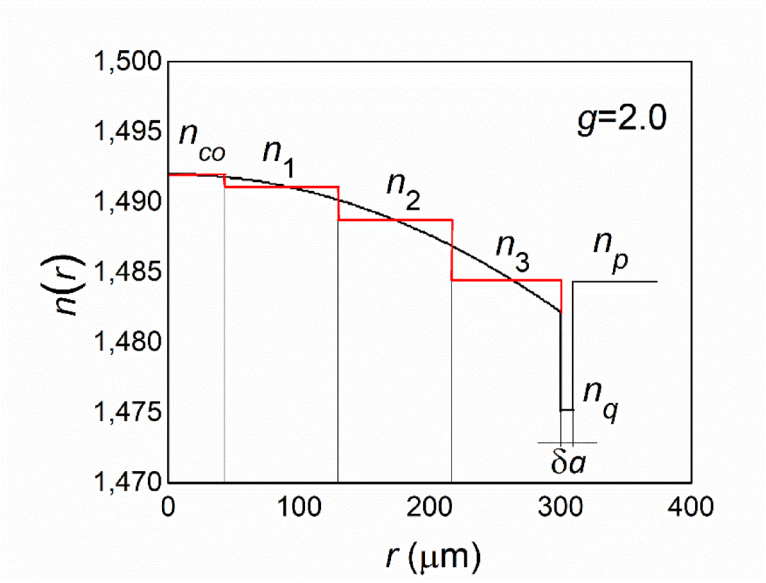

(b)

Fig. 1. (**a**) A quarter cross-section of the multimode W-type GI mPOF. The pitch Λ determines the position of air-holes with diameters d_1, d_2, d_3, d_p and d_q in a triangular lattice, (**b**) The solid black line represents the RI distribution of W-type GI mPOF, for $g = 2.0$, at $\lambda = 645$ nm.

$$\alpha_{\mathrm{L}}(m,\lambda)=\frac{4\sqrt{2\Delta_q}\left(\left(\frac{m}{m_q}\right)^{\frac{2g}{g+2}}-\left(\frac{m_p}{m_q}\right)^{\frac{2g}{g+2}}\right)^{1/2}}{a\left(1-2\Delta_q\left(\frac{m}{m_q}\right)^{\frac{2g}{g+2}}\right)^{1/2}}\frac{\left(\frac{m}{m_q}\right)^{\frac{2g}{g+2}}\left(1-\left(\frac{m}{m_q}\right)^{\frac{2g}{g+2}}\right)}{\left(1-\frac{\Delta_p}{\Delta_q}\left(\frac{m_p}{m_q}\right)^{\frac{2g}{g+2}}\right)}\exp\left[-2\delta a n_{co}k\left(2\Delta_q\left(1-\left(\frac{m}{m_q}\right)^{\frac{2g}{g+2}}\right)\right)^{1/2}\right] \tag{5}$$

where m_p is given as $m_p=\sqrt{g\Delta_p(\lambda)/(g+2)}akn_{co}(\lambda)$. The modal attenuation in a W-type GI optical fiber can be expressed as:

$$\alpha_d(m,\lambda)=\begin{cases}0 & m\leqslant m_{\mathrm{p}}\\ \alpha_{\mathrm{L}}(m,\lambda) & m_{\mathrm{p}}<m<m_{\mathrm{q}}\\ \infty & m\geqslant m_{\mathrm{q}}\end{cases} \tag{6}$$

Because of the strong dependence of $\alpha_L(m)$ on the intermediate layer width δa (Eq. 5), it is expected that characteristics of a W-type GI mPOF also strongly depend on δa[9,24,25]. We solved Eq. (1) using the explicit finite difference method (EFDM). As first in the authors' best knowledge, numerical solution of the TI PFE (1) is reported in this work for investigation of the transmission along a newly designed W-type GI mPOF.

Time-dependent PFE

Time-dependent (TD) PFE for multimode optical fibers with GI core distribution is:

$$\begin{aligned}&\frac{\partial P(m,\lambda,z,\omega)}{\partial z}+j\omega\tau(m,\lambda)P(m,\lambda,z,\omega)=-\alpha(m,\lambda)P(m,\lambda,z,\omega)\\&+\frac{\partial P(m,\lambda,z,\omega)}{\partial m}\frac{\partial d(m,\lambda)}{\partial m}+d(m,\lambda)\frac{1}{m}\frac{\partial P(m,\lambda,z,\omega)}{\partial m}+d(m,\lambda)\frac{\partial P^2(m,\lambda,z,\omega)}{\partial m^2}\end{aligned} \tag{7}$$

where $P(m,\lambda,z,\omega)$ is power in the m-the principal mode, z is coordinate along the fiber axis from the input fiber end, $\alpha(m,\lambda)$ is attenuation of the mode m (Eq. (6)), $d(m,\lambda)$ is the coupling coefficient of the mode m (assumed constant D), $\omega=2\pi f$ is the baseband angular frequency, $\tau(m,\lambda)$ is delay time per unit length of mode m, given as:

$$\tau(m,\lambda)\cong\frac{n_{co}(\lambda)}{c}\left[1+\frac{g-2}{g+2}\Delta_q(\lambda)\left(\frac{m}{M(\lambda)}\right)^{2g/(g+2)}+\frac{1}{2}\frac{3g-2}{g+2}\Delta_q(\lambda)^2\left(\frac{m}{M(\lambda)}\right)^{4g/(g+2)}\right] \tag{8}$$

where c is the free-space velocity of light. We solved Eq. (8) using the EFDM.

Numerical results and discussion

Light transmission was examined in a multimode W-type GI mPOF (Fig. 1), for which the effective V parameter can be written as:

$$V=\frac{2\pi}{\lambda}a_{eff}\sqrt{n_{co}^2-n_{fsm}^2} \tag{9}$$

where $a_{\mathrm{eff}}=\Lambda/\sqrt{3}$ is the effective core radius[26], and n_{fsm} is the effective RI for various core and cladding layers, as determined by combining the Eq. (9) with the effective V parameter[26]:

$$V\left(\frac{\lambda}{\Lambda},\frac{d}{\Lambda}\right)=A_1+\frac{A_2}{1+A_3\exp\left(A_4\lambda/\Lambda\right)} \tag{10}$$

The fitting parameters A_{i} (i = 1 to 4) are given as:

$$A_i=a_{i0}+a_{i1}\left(\frac{d}{\Lambda}\right)^{b_{i1}}+a_{i2}\left(\frac{d}{\Lambda}\right)^{b_{i2}}+a_{i3}\left(\frac{d}{\Lambda}\right)^{b_{i3}} \tag{11}$$

The coefficients a_{i0} to a_{i3} and b_{i1} to b_{i3} (i = 1 to 4) are given in our previous work[16].

The characteristics of W-type GI mPOF analyzed in this work are: The core radius of the fiber is $a=300$ µm, the RI of the core at the fiber axis was $n_{co}=1.4920$ at wavelength $\lambda=645$ nm. For pitch $\Lambda=3$ µm and air-hole diameters of the five air-hole rings $d_1=0.3$ µm, $d_2=0.5$ µm, $d_3=1.0$ µm, d_p=1.0 µm and d_q=1.5 µm, using Eqs. (10) and (11), we obtain the refractive indices $n_1=1.4907$, $n_2=1.4887$, $n_3=1.4884$ and n_p=1.4844 and n_q=1.4757, respectively (material dispersion has also been taken into account). For the investigated fiber, the maximum principal mode number is $M=322$, $g=2.0$ and $\Delta_q=(n_{co}-n_q)/n_{co}$=0.0109. The normalized intermediate layer widths $\delta=0.008$ and $\delta=0.024$ were employed (actual width is $\delta\cdot a$ [µm]). The constant coupling coefficient $D=1482\ 1/\mathrm{m}$[14] and wavelength $\lambda=645$ nm were used in the calculations. By numerical solving the TI PFE (1), we calculated the length L_c at which the EMD is achieved and length z_s at which the SSD is established in W-type GI mPOF. Figure 2 shows the output modal power distribution in W-type GI mPOF with the width of the intermediate layer $\delta=0.008$ at different lengths. In the numerical calculations, a Gaussian LBD $P(\theta,z)$ is assumed to be launched with $<\theta>=0°$ and full width at half maximum $(\mathrm{FWHM})_0=3°$. Results are shown for five different radial offsets Δr = 0, 100, 150, 200 and 250 µm. As additional illustration, Fig. 3 shows calculated

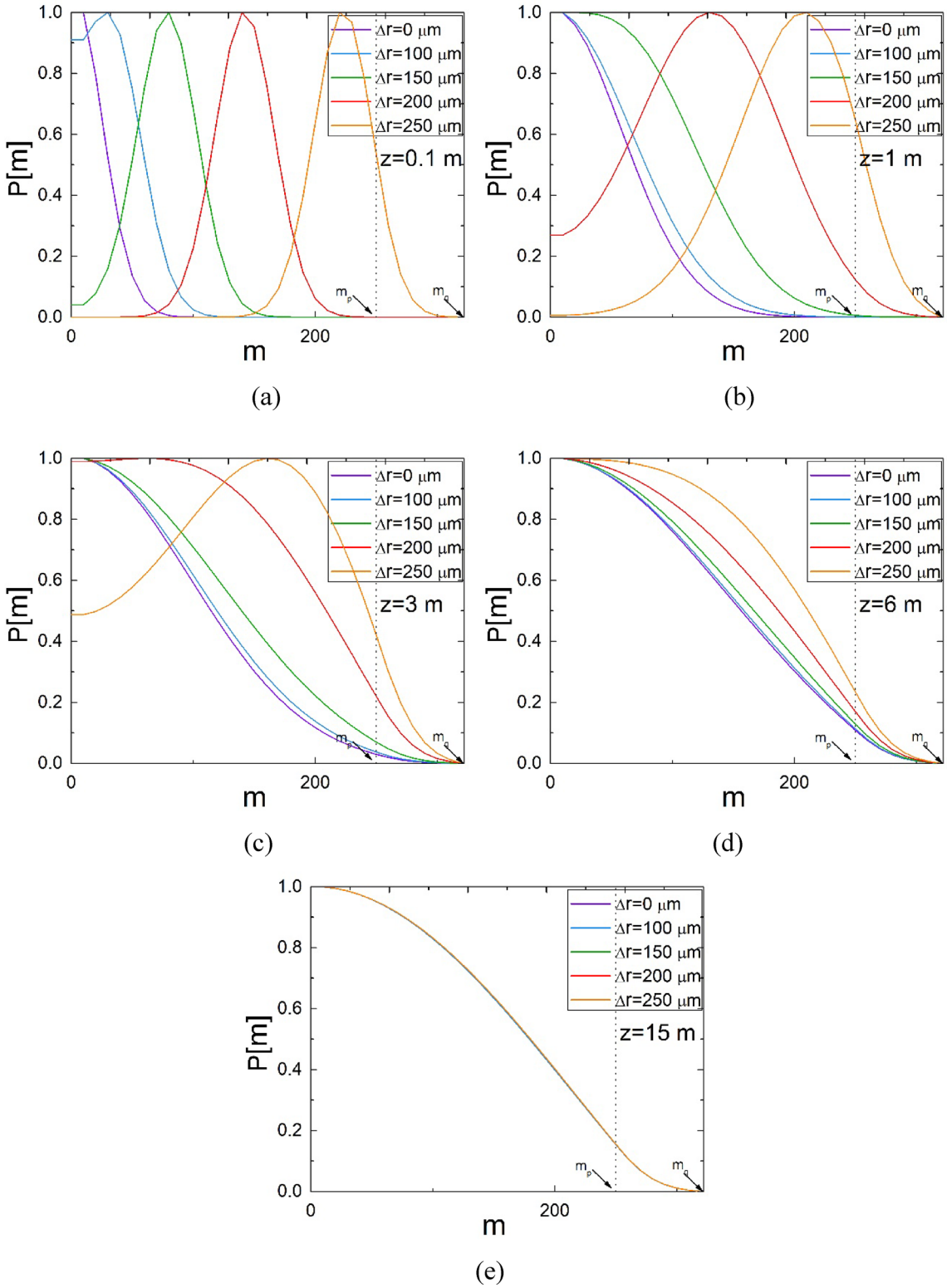

Fig. 2. Calculated output modal power distribution $P(m)$ in W-type GI mPOF with $\delta = 0.008$, over a range of radial offsets Δr, at fiber lengths (**a**) $z = 0.1$ m, (**b**) $z = 1$ m, (**c**) $z = 3$ m, (**d**) $z = 6$ m and (**e**) $z = 15$ m, for Gaussian launch beam distribution with $(\theta) = 0°$ and $(\mathrm{FWHM})_0 = 3°$.

3-dim output modal power distribution with radial offsets $\Delta r = 0\ \mu$m at different fiber lengths. One can see from Fig. 2 that for $\delta = 0.008$, the EMD and SSD in W-type GI mPOF are achieved at fiber length L_c=6 m and z_s=15 m, respectively. For $\delta = 0.024$, these lengths are L_c=7 m and z_s=18 m, respectively (Table 1). For comparison, the EMD in SC GI POF experimentally investigated in our earlier work was achieved at L_c = 31 m (for SC GI

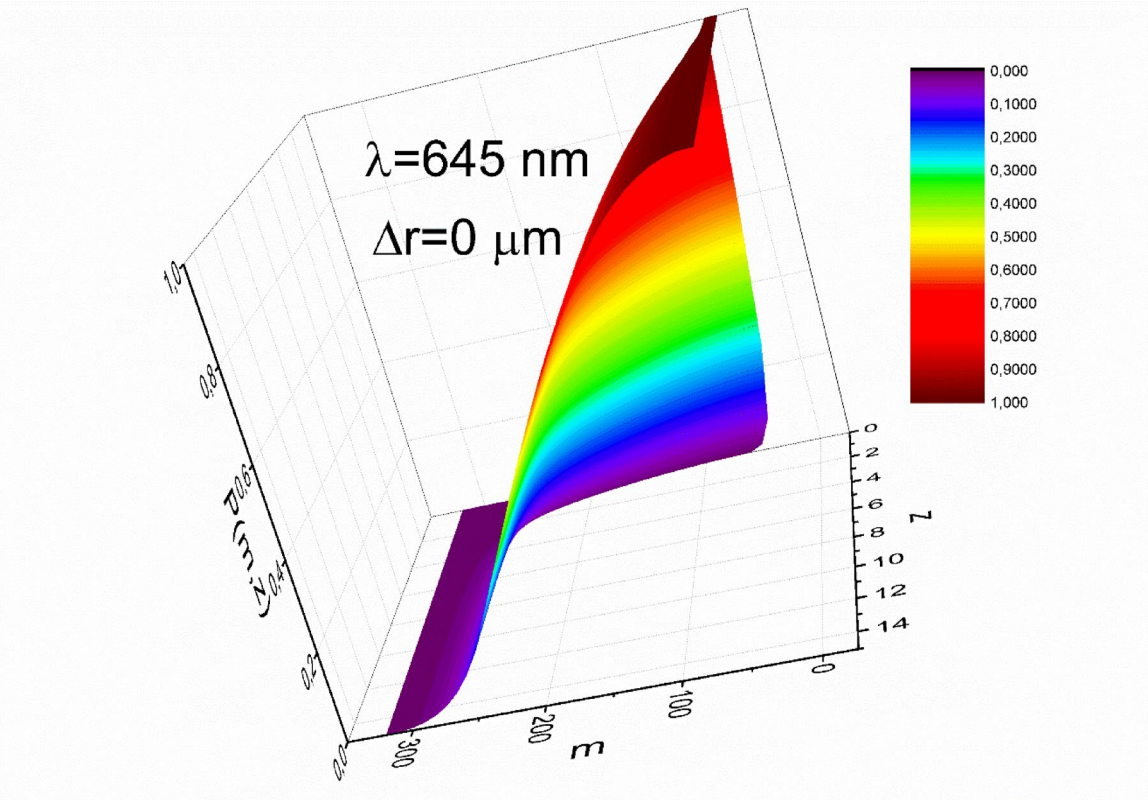

Fig. 3. Calculated 3-dim output modal power distribution $P(m)$ in W-type GI mPOF with $\delta = 0.008$, for Gaussian launch beam distribution with radial offsets $\Delta r = 0\ \mu$ m, $< \theta > = 0°$ and $(\mathrm{FWHM})_0 = 3°$, at different fiber lengths.

$(\mathrm{FWHM})_0 = 3°$	L_c (m)	z_s (m)
$\delta = 0.008$	6	15
$\delta = 0.024$	7	18

Table 1. Coupling length L_c (for EMD) and length z_s (for SSD) in W-type GI mPOF with different widths of the intermediate layer δ, for the launch beam distribution with $(\mathrm{FWHM})_0 = 3°$.

POF, $M = 656$ and $D = 1482\ \ 1/\mathrm{m}$)[14]. The length L_c is lowered in the case of W-type GI mPOF due to a decrease in the number of higher guided modes engaged in the coupling process. With increasing the width of the inner cladding of W-type GI mPOF, leaky mode losses reduce (number of guided modes increases), leading to longer lengths L_c and z_s in the case $\delta = 0.024$.

We determined the bandwidth for the investigated W-type GI mPOF using the TD PFE. Figure 4 shows that, for short lengths, bandwidth drops linearly before switching to the $1/z^{1/2}$ functional dependence. With thinner intermediary layers, this changeover and the ensuing EMD happen at shorter fiber lengths. The faster bandwidth increase happens, the shorter L_c. It is also important to note that the larger leaky mode losses (fewer higher guided modes) in the case of the thinner intermediary layer leads to smaller modal dispersion and larger bandwidth. When compared to the bandwidth of the conventional SC GI POF (Fig. 5)[18], the W-type GI mPOF examined in this work has a substantially larger bandwidth. Namely, in the proposed W-type GI mPOF, higher guided modes are filtered out, resulting in diminished modal dispersion. This is a result of the proposed W-type GI mPOF in which a higher guided modes are attenuated, leading to reduced modal dispersion. As shown in Fig. 4, at short fiber lengths, the bandwidth decreases with increasing radial offset. This is due to greater modal dispersion resulting from the initial excitation of higher-order guided modes in the case of larger radial offset. However, this effect diminishes over longer fiber lengths as a result of mode coupling. Such newly designed W-type GI mPOF is a promising candidate for a high bandwidth performance of short distance communication links.

It is important to note here that, in general, mode coupling arises due to random perturbations and the propagation constant difference ($\Delta\beta$) between modes, with $\Delta\beta$ determining the coupling strength. The smaller $\Delta\beta$, the stronger the coupling. More modes mean that the effective refractive index difference ($\Delta\beta$) of adjacent modes may decrease, resulting in enhanced coupling. In fact, for multimode fiber, the average coupling

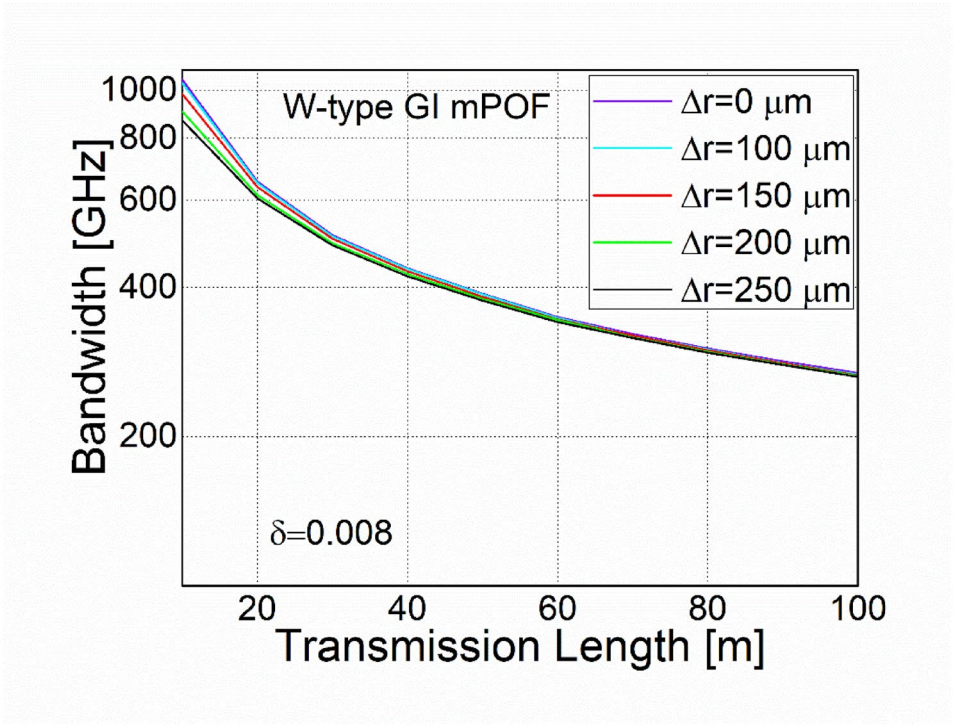

(a)

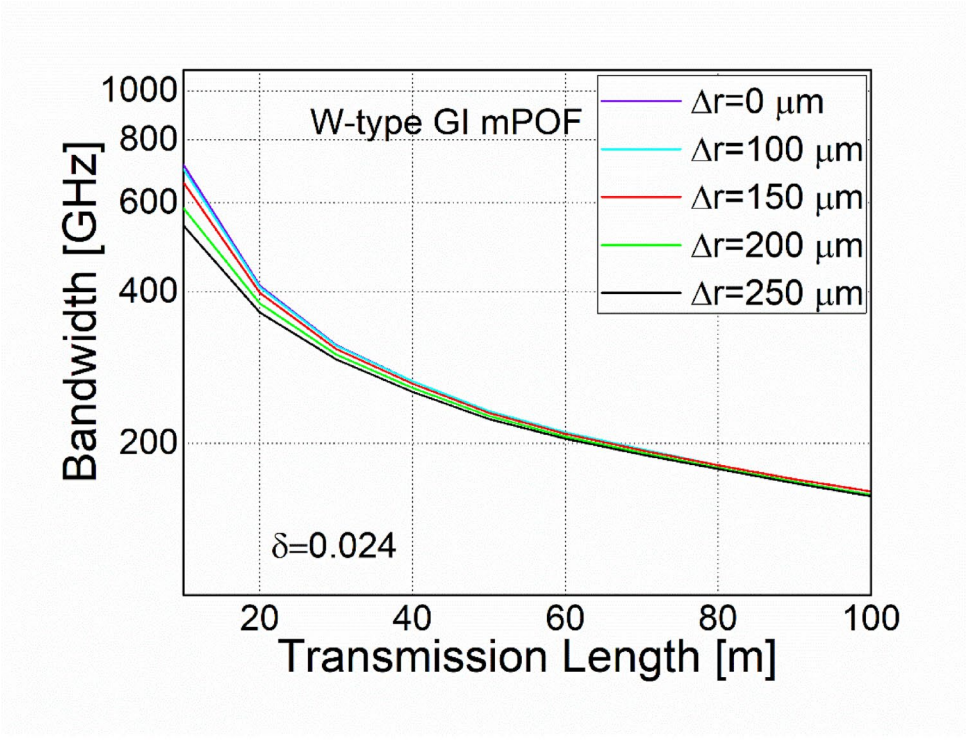

(b)

Fig. 4. Bandwidth versus transmission length in the W-type GI mPOF with (**a**) $\delta = 0.008$ and (**b**) $\delta = 0.024$, for a various radial offsets Δr and Gaussian launch beam distribution with $< \theta > = 0°$ and $(\mathrm{FWHM})_0 = 3°$.

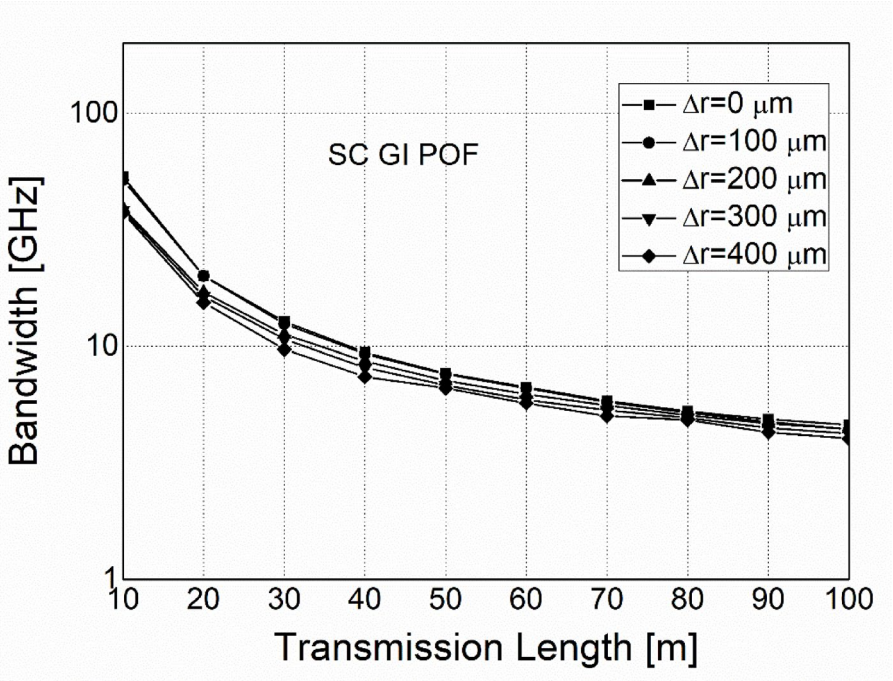

Fig. 5. Measured bandwidth versus transmission length in the conventional SC GI POF for a various radial offsets Δr and Gaussian launch beam distribution with $< \theta > = 0°$ and $(FWHM)_0 = 3°$ (lines are drawn to guide the eye)[18].

length decreases as the number of modes increases. Therefore, only by reducing the number of modes can the length (perturbation period) $l_c \sim 1/(\Delta\beta)$ be increased. For example, in the weak coupling regime (few-mode fiber), l_c can reach several kilometers. In the strong coupling regime (multimode fiber), l_c may drop to the centimeter level. For space division multiplexing (SDM) systems, there is a trade-off between transmission capacity and crosstalk. A high number of modes can improve the spatial multiplexing rate, but shortening l_c will increase the crosstalk between modes. Similarly, increasing l_c will reduce the crosstalk between modes, but will reduce the spatial multiplexing rate. Low crosstalk requires $L \ll l_c$ (L is the transmission distance). This has been demonstrated in our previous works for POFs, where L is only few meters for three spatially multiplexed channels and 10 m for two spatially multiplexed channels[27,28]. Otherwise digital signal processing compensation is required, which increases the complexity. Another, and potentially superior, SDM solution is the design of a multicore optical fiber, but this requires careful consideration of inter-core crosstalk[29–31].

Conclusion

A novel multimode W-type GI mPOF was proposed, and we presented a methodology for examining its transmission. Our findings indicate that the coupling length L_c required to generate an EMD in W-type GI mPOF is less than the length found in the experiment with conventional SC GI POF. The reduction in the number of higher guided modes involved in the coupling process, as a result of leaky mode losses, lowers the length L_c. In W-type GI mPOF, fewer higher guided modes result in a lower modal dispersion and a higher bandwidth. Thinner intermediate layers are proven to further boost bandwidth. This study's analysis of the W-type GI mPOF indicates a much higher bandwidth when compared to commercially available conventional POFs. Bandwidth decreases as the radial offset increases, primarily due to increased modal dispersion caused by the initial excitation of higher-order guided modes. However, this effect becomes negligible over longer fiber lengths due to mode coupling. Consequently, a large gain in bandwidth performance in short-distance communication lines may be possible with such a W-type GI mPOF architecture.

Data availability

The data presented in this study are available on request from the corresponding author.

Received: 5 March 2025; Accepted: 6 May 2025
Published online: 16 May 2025

References

1. Patel, K. M. & Ralph, S. E. Enhanced multimode fiber link performance using a spatially resolved receiver. *IEEE Photon Technol. Lett.* **14**, 393–395 (2002).
2. Tyler, E. J. et al. Subcarrier modulated transmission of 2.5 Gb/s over 300 m of 62.5-μm-core diameter multimode fiber. *IEEE Photon Technol. Lett.* **14**, 1743–1745 (2002).

3. Zhao, X. & Choa, F. S. Demonstration of 10 Gb/s transmission over 1.5-km-long multimode fiber using equalization techniques. *IEEE Photon Technol. Lett.* **14**, 1187–1189 (2002).
4. Abbott, J. S., Smith, G. E. & Truesdale, C. M. *Multimode fiber Link. Dispersion Compensator*. U S Patent 6 363 195 (2002).
5. Yamashita, T. & Kagami, M. Fabrication of light-induced self-written waveguides with a W-shaped refractive index profile. *J. Lightwave Technol.* **23**, 2542–2548 (2005).
6. Asai, M., Inuzuka, Y., Koike, K., Takahashi, S. & Koike, Y. High-bandwidth graded-index plastic optical fiber with low-attenuation, high-bending ability, and high-thermal stability for home-networks. *J. Lightvawe Technol.* **29**, 1620–1626 (2011).
7. Mikoshiba, K. & Kajioka, H. Transmission characteristics of multimode W-type optical fiber: experimental study of the effect of the intermediate layer. *Appl. Opt.* **17**, 2836–2841 (1978).
8. Takahashi, K., Ishigure, T. & Koike, Y. Index profile design for high-bandwidth W-shaped plastic optical fiber. *J. Lightwave Technol.* **24**, 2867–2876 (2006).
9. Tanaka, T., Yamada, S., Sumi, M. & Mikoshiba, K. Microbending losses of doubly clad (W-type) optical fibers. *Appl. Opt.* **18**, 2391–2394 (1977).
10. Babita, V. R. & Kumar, A. Design of large-mode-area three layered fiber structure for femtosecond laser pulse delivery. *Opt. Commun.* **293**, 108–112 (2013).
11. Simović, A., Savović, S., Drljača, B. & Djordjevich, A. Influence of the fiber design and launch beam on transmission characteristics of W-type optical fibers. *Opt. Laser Technol.* **68**, 151–159 (2015).
12. Savović, S., Simović, A. & Djordjevich, A. Explicit finite difference solution of the power flow equation in W-type optical fibers. *Opt. Laser Techn*. **44**, 1786–1790 (2012).
13. Kitayama, K., Seikai, S. & Uchida, N. Impulse response prediction based on experimental mode coupling coefficient in a 10-km long graded-index fiber. *IEEE J. Quant. Electron.* **16**, 356–362 (1980).
14. Savović, S. et al. Power flow in graded index plastic optical fibers. *J. Lightwave Technol.* **37**, 4985–4990 (2019).
15. Yabre, G. Comprehensive theory of dispersion in graded-index optical fibers. *J. Lightwave Technol.* **18**, 166–177 (2000).
16. Savović, S. et al. Method for investigation of mode coupling in multimode step-index silica photonic crystal fibers. *Optik* **246**, 167728 (2021).
17. Drljača, B. et al. Theoretical investigation of bandwidth of multimode step-index silica photonic crystal fibers. *Photonics* **9** (4), 214 (2022).
18. Simović, A., Djordjevich, A., Drljača, B., Savović, S. & Min, R. Investigation of bandwidth in multimode graded index plastic optical fibers. *Opt. Express*. **29**, 29587–29594 (2021).
19. Koike, Y. & Koike, K. Progress in low-loss and high-bandwidth plastic optical fibers. *J. Polym. Sci. B.* **49**, 2–17 (2011).
20. Simović, A., Savović, S., Drljača, B. & Djordjevich, A. Enhanced bandwidth of W type plastic optical fibers designed from single clad step index plastic optical fibers. *Opt. Laser Technol.* **111**, 629–634 (2019).
21. Olshansky, R. Mode coupling effects in graded-index optical fibers. *Appl. Opt.* **14**, 935–945 (1975).
22. Nagano, K. & Kawakami, S. Measurements of mode conversion coefficients in graded-index fibers. *Appl. Opt.* **19**, 2426–2434 (1980).
23. Simović, A., Savović, S., Drljača, B., Djordjevich, A. & Min, R. Theoretical investigation of the influence of wavelength on the bandwidth in multimode W-type plastic optical fibers with graded index core distribution. *Polymers* **13**, 3973 (2021).
24. Ishigure, T. Modal bandwidth enhancement in a plastic optical fiber by W-refractive index profile. *J. Lightwave Technol.* **23**, 1754–1762 (2005). H. Endo, K. Ohdoko, K. Takahashi, and Y. Koike.
25. Drljača, B. et al. Transmission performance of multimode W-type microstructured polymer optical fibers. *Opt. Express*. **30**, 24667–24675 (2022).
26. Saitoh, K. & Koshiba, M. Empirical relations for simple design of photonic crystal fibers. *Opt. Express*. **13** (1), 267–274 (2005).
27. Savović, S., Djordjevich, A., Simović, A. & Drljača, B. Influence of mode coupling on three spatially multiplexed channels in multimode graded index plastic optical fibers. *Laser Phys.* **30**, 115102 (2020).
28. Savović, S., Aidinis, K., Chen, C. & Min, R. Theoretical investigation of the space division multiplexing in multimode step-index plastic optical fibers. *Optik* **311**, 171945 (2024).
29. Koshiba, M. & Saitoh, K. Crosstalk behaviors in multicore fibers under deployed conditions: role of structural fluctuations. *IEEE Photonics Technol. Lett.* **37**, 353–356 (2025).
30. Chen, W. et al. Applications and development of multi-core optical fibers. *Photonics* **11**, 270 (2024).
31. Savović, S., Djordjevich, A., Aidinis, K. & Min, R. Influence of the width of launch beam distribution on the transmission performance of seven-core plastic-clad silica fibers. *Photonics* **9**, 645 (2022).

Author contributions

S.S., A.S., B.D., A.Dj., and K.A.-Conceptualization; S.S., A.S., B.D., C.Y., and K.A.-Methodology; A.S., B.D., M.S.K., and Lj.K.-Software; C.Y., X.D., and S.S.-Validation; A.S., S.S., K.A., and C.Y._Visualization; A.S., B.D., M.S.K., Lj.K., and A.Dj.-Writing original manuscript; S.S., K.A., C.Y., X.D., and A.Dj.-Writing rewiv and editing; S.S.-Supervision; S.S., K.A, X.D., and C.Y.-Project administration and funding.

Funding

A Funding for this study is provided by the grants from Serbian Ministry of Science, Technological Development, and Innovations (Agreement No. 451-03-137/2025-03/200122; 451-03-65/2024-03/200123); by the grants from National Natural Science Foundation of China (62001174) and Sichuan Outstanding Youth Science and Technology Talents Project (2022JDJQ0047); and by the grants from Ajman University (Grant ID: 2023-IRG-ENIT-14; 2024-IRG-ENIT-10).

Declarations

Competing interests

The authors declare no competing interests.

Additional information

Correspondence and requests for materials should be addressed to S.S.

Reprints and permissions information is available at www.nature.com/reprints.

Publisher's note Springer Nature remains neutral with regard to jurisdictional claims in published maps and institutional affiliations.